Proc. Natl. Acad. Sci. USA
Vol. 96, pp. 7780–7784, July 1999
Biochemistry

The γ-subunit rotation and torque generation in F_1-ATPase from wild-type or uncoupled mutant *Escherichia coli*

(ATP synthase/rotational catalysis/frictional torque)

HIROSHI OMOTE*, NORIKO SAMBONMATSU*, KIWAMU SAITO†, YOSHIHIRO SAMBONGI*, ATSUKO IWAMOTO-KIHARA‡, TOSHIO YANAGIDA§, YOH WADA*, AND MASAMITSU FUTAI*¶

*Division of Biological Sciences, Institute of Scientific and Industrial Research, Osaka University, CREST of Japan Science and Technology Corporation, Ibaraki, Osaka 567-0047, Japan; †Department of Physics, Kanazawa University, Kanazawa 920-1192, Japan; ‡Department of Biology, Graduate School of Arts and Sciences, University of Tokyo, Komaba, Tokyo 153-8902, Japan; and §Department of Physiology, Osaka University Medical School, Suita, Osaka 565-0871, Japan

Communicated by Paul D. Boyer, University of California, Los Angeles, CA, April 28, 1999 (received for review March 11, 1999)

ABSTRACT **The rotation of the γ-subunit has been included in the binding-change mechanism of ATP synthesis/hydrolysis by the proton ATP synthase (F_OF_1). The *Escherichia coli* ATP synthase was engineered for rotation studies such that its ATP hydrolysis and synthesis activity is similar to that of wild type. A fluorescently labeled actin filament connected to the γ-subunit of the F_1 sector rotated on addition of ATP. This progress enabled us to analyze the γM23K (the γ-subunit Met-23 replaced by Lys) mutant, which is defective in energy coupling between catalysis and proton translocation. We found that the F_1 sector produced essentially the same frictional torque, regardless of the mutation. These results suggest that the γM23K mutant is defective in the transformation of the mechanical work into proton translocation or vice versa.**

The ATP synthases (F_OF_1) of mitochondria, chloroplasts, and *Escherichia coli* synthesize ATP coupled with an electrochemical gradient of protons (for reviews, see refs. 1–6). The conserved basic structure of the enzyme consists of a catalytic sector, F_1 or F_1-ATPase ($\alpha 3\beta 3\gamma 1\delta 1\varepsilon 1$), and a proton pathway, F_O ($a1b2c12$). The crystal structure of the bovine $\alpha 3\beta 3\gamma$ complex indicates that the α- and β-subunits are arranged alternately around the amino- and carboxyl-terminal α-helices of the γ-subunit (7). Catalytic sites are mostly comprised of residues from the β-subunit. These catalytic sites participate alternately in ATP synthesis as predicted by the binding-change mechanism (5). Consistent with this mechanism, the three β-subunits in the bovine structure have different conformations: empty, ATP-bound, and ADP-bound forms (7). "Conformation transmission successively among three β subunits through the mechanical γ subunit rotation" (5) has been a fascinating model to include in the binding-change mechanism. The γ-subunit rotation has been suggested by cryo-electron microscopy studies of F_1 (8), chemical cross-linking experiments on the subunits (9, 10), and analysis of polarized absorption recovery after photobleaching of a probe linked to the γ-subunit (11, 12). Finally, the rotation of an actin filament attached to a thermophilic bacterial γ-subunit was observed directly and video-recorded (13). Thus, ATP synthesis or hydrolysis is a combination of three different steps: catalysis, mechanical work (γ-subunit rotation and torque generation), and proton transport. During proton transport, rotational movement of the *c* subunit oligomer (a group of 12 *c* subunits) has also been proposed (5, 12, 14).

The energy coupling of the three steps can be analyzed, taking advantage of the wealth of information on the *E. coli* ATP synthase accumulated through the combined biochemical and genetic approaches. Furthermore, mutants can be easily isolated by using a plasmid carrying the *unc* (or *atp*) operon for F_OF_1, and their ATP synthesis, hydrolysis, and proton translocation can be readily assayed (15, 16). Mutants mapped at or near the catalytic site (15–20) or those defective in energy coupling (21–26) may be useful for defining the mechanical-work step during ATP synthesis or hydrolysis. Thus, it is important to establish an assay system for observing the mechanical work of the *E. coli* γ-subunit.

In this study, we observed that an actin filament connected to the *E. coli* γ-subunit could rotate by using the energy of ATP hydrolysis. With this progress, we could analyze the energy-coupling mutant, γM23K (γ-subunit Met-23 replaced by Lys), of which F_OF_1 shows low ATP-driven proton transport and ATP synthesis (22–25). We found that the mutant γ-subunit could generate essentially the same torque as that of the wild-type subunit. Thus, the major defect of the γM23K mutant is in the transformation of mechanical work into proton transport.

EXPERIMENTAL PROCEDURES

Bacterial Strain, Growth Conditions, and Plasmids. *E. coli* strain DK8 (27) lacking all genes for ATP synthase (Δ*unc*) was used as a host for recombinant plasmids and grown at 37°C in a rich medium (L broth) supplemented with ampicillin or a synthetic medium with 0.5% glycerol (15). The *unc* operon bearing plasmids pBWU17 (28) and pBMUG420-γM23K (*unc* operon plasmid with the γM23K mutation; A.I.-K., unpublished work) was used.

Construction of *unc* Operon Plasmids Carrying a His-tag and γ-Subunit Ser-193 to Cys Replacement. Codons for the $Met(His)_6$ sequence (His-tag) were introduced in front of the initiation codon of the α- or β-subunit gene carried by pBWU17; a double-stranded cassette [5′-CAT(CAC)5ATG-3′/3′-GTACGTA(GTG)4GT-5′] was introduced into a *Sph*I site located in the initiation codon of the α-subunit. For the β-subunit, the *Sph*I–*Nar*I fragment (60-bp upstream sequence from the βGly-10 codon) was replaced with a similar cassette for $Met(His)_6$ and then introduced into pBWU17. To construct a γSer-193 to Cys substitution of the γ-subunit, the *Sal*I–*Spe*I segment was cloned; the γS193C (TCA → TGC) substitution was introduced into the segment by PCR; and the *Rsr*II–*Spe*I segment with the substitution was introduced into pBWU17 engineered with a His-tag. The γM23K mutation was introduced by replacing *Csp*45I–*Rsr*II (with *unc* operon segment between the αPhe-467 and γIle-149 codons) of the engineered plasmid with the corresponding fragment from pBMUG420–γM23K.

Preparation of F_1-ATPase. Membrane vesicles were prepared from cells grown on 0.5% glycerol, suspended in 20 mM

The publication costs of this article were defrayed in part by page charge payment. This article must therefore be hereby marked "*advertisement*" in accordance with 18 U.S.C. §1734 solely to indicate this fact.

PNAS is available online at www.pnas.org.

¶To whom reprint requests should be addressed. e-mail: m-futai@sanken.osaka-u.ac.jp.

Tris·HCl buffer (pH 8.0) containing 0.5 mM DTT, 140 mM KCl, 1 mM EDTA, and 10% (wt/vol) glycerol, and then centrifuged at 160,000 × *g* for 1 h to remove the δ-subunit. The precipitate was incubated in 2 mM Tris·HCl (pH 8.0) containing 1 mM EDTA for 10 min. After centrifugation, 1 M Hepes-NaOH (pH 7.8) and 1 M $MgSO_4$ were added to the supernatant (final concentrations of 50 mM and 2 mM, respectively), and the mixture was incubated with 100 μM biotin-$PEAC_5$-maleimide (Dojindo, Kumamoto, Japan) for 30 min. The mixture was applied to a ≈10–30% (wt/vol) glycerol gradient [containing 10 mM Hepes-NaOH (pH 7.8) and 2 mM $MgSO_4$] and then centrifuged at 350,000 × *g* for 4 h. The essentially pure biotinylated F_1-ATPase was obtained in the fractions containing 20–25% (wt/vol) glycerol. All solutions contained 0.5 mM PMSF, 5 μg/ml leupeptin, and 5 μg/ml pepstatin, except that PMSF was omitted from the glycerol gradient.

Assaying Actin Filament Rotation. Rotation was assayed by the slightly modified method previously reported (13). Buffer A (10 mM Hepes-NaOH, pH 7.2/25 mM KCl/5 mM $MgCl_2$/10 mg/ml BSA) was included in all solutions used, unless otherwise specified. A flow cell ≈20–50 μm deep was constructed from nitrocellulose-coated cover glass by using Parafilm (American National Can, Chicago, IL) and filled with 0.8 μM Ni-NTA HRP Conjugate (Qiagen, Germany) in buffer A without BSA. After a 5-min incubation at 25°C with Ni-NTA HRP Conjugate, 10 mg/ml BSA, 10 nM F_1-ATPase, and 4 μM streptavidin were successively introduced into the flow cell and incubated for 5 min after each addition. Fluorescently labeled actin filament (12.5 nM) and 0.1 mM biotin were added to construct F_1-ATPase with an attached actin filament, and finally the reaction mixture for rotation (50 μM to 5 mM Mg-ATP/1 μM biotin/50 μg/ml pyruvate kinase/1 mM phospho*enol* pyruvate/25 mM glucose/1% β-mercaptoethanol/216 μg/ml glucose oxidase/36 μg/ml catalase in buffer A) was introduced into the flow cell. The cell was sealed with silicon grease, and the rotations were observed at 25°C by using a Zeiss Axiovert 135 equipped with an ICCD camera (Atto Instruments, Rockville MD) and video-recorded. The rotation angle of the filament was estimated from the centroid of the actin filament. Rotation (revolutions per second) was calculated from the slope of the curves, as shown in Fig. 1.

Other Procedures. ATPase activity and the formation of an electrochemical proton gradient were assayed under the conditions used for the rotation assay. The measurement of protein concentrations and other procedures were performed as described (15, 21).

Materials. Actin filament and biotin-$PEAC_5$-maleimide were incubated in a molar ratio of 1:5 at 25°C for 1 h. Biotinylated actin filaments were mixed with an equal amount of native actin and then labeled with phalloidin tetramethyl rhodamine as described (29). DNA-modifying enzymes were obtained from Takara Shuzo (Kyoto) or New England Biolabs. Other chemicals used were of the highest grade commercially available.

RESULTS

Engineering of *E. coli* F_1-ATPase. A cluster of His residues was introduced into the α- or β-subunit amino terminus to immobilize F_1-ATPase on a glass surface, and γSer-193 was replaced with a Cys residue to attach the actin filament. We

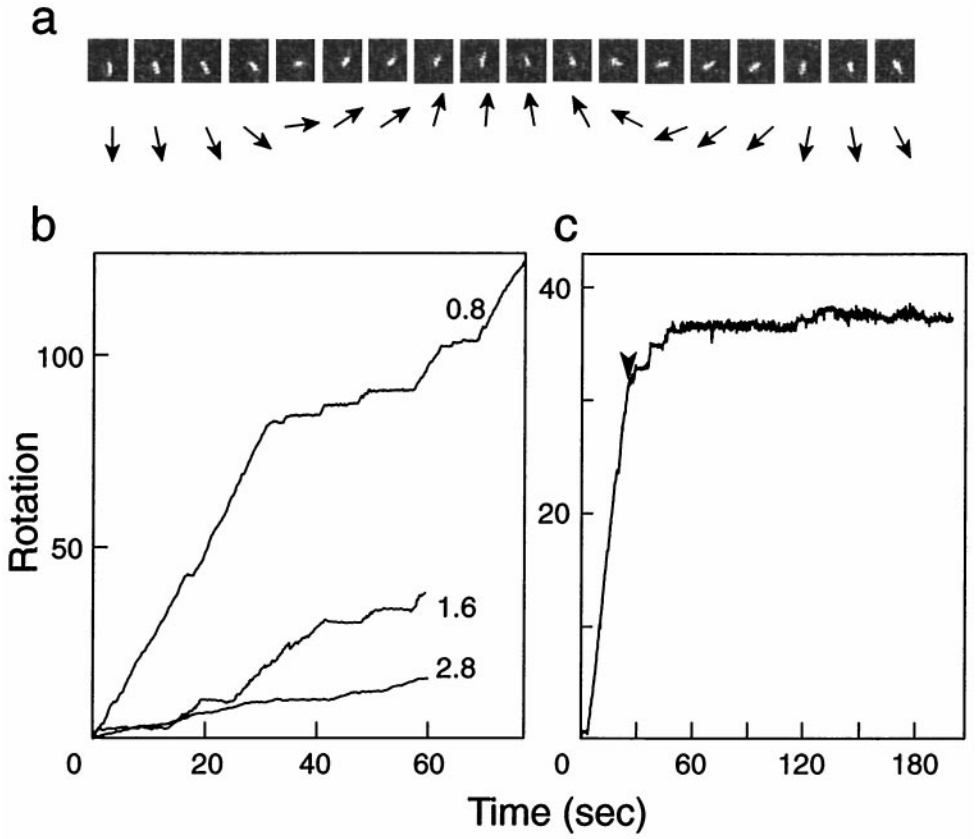

FIG. 1. Rotation of an actin filament attached to the γ-subunit of *E. coli* F_1-ATPase. (*a*) Typical sequential video images (left to right) of a rotating actin filament attached to the engineered enzyme (αHis-tag/γSer193Cys) in 5 mM Mg-ATP; the filament length between rotation axis and the tip was 2.1 μm, and the image interval was 100 msec. The directions of the actin filaments are shown schematically by arrows below the video images. (*b*) Examples of the rotation of actin filaments dependent on time. The rotations of actin filaments (0.8, 1.6, and 2.8 μm) were followed in the presence of 5 mM Mg-ATP. (*c*) Effect of azide on the rotation of a 2.0-μm actin filament. A reaction mixture containing 1 mM sodium azide was slowly (≈2 μl/sec) introduced into the cell at the time indicated by the arrowhead.

selected γSer-193 because the corresponding chloroplast residue is in the domain that is accessible to ferredoxin with light (30). The engineered enzyme with αHis-tag/γS193C had similar ATPase activity to the wild type and supported growth by oxidative phosphorylation (data not shown). The specific activity of the purified F_1-ATPase was essentially the same as that of the enzyme before engineering (Table 1). For detailed studies, it is desirable that mutations can be introduced into the engineered enzyme without affecting the subunit assembly. The γ-subunit γM23K substitution could be introduced into the enzyme without substantial effects on the assembly or ATPase activity: the mutant F_1-ATPase activity was about 60% of that of the wild type (Table 1).

We also constructed αHis-tag/γK108C and βHis-tag/γS193C enzymes. However, these enzymes were difficult to purify, especially when the γM23K substitution was introduced. Thus the enzyme with αHis-tag/γS193C was used throughout this study. It should be noted that a His-tag was introduced into the β-subunit of the thermophilic enzyme (13).

Observing Rotation. The engineered enzyme was biotinylated at γCys-193, which was linked with an actin filament connected through streptavidin. The enzyme was fixed on the Ni-NTA-coated glass surface through the His-tag. With the addition of a steady-state concentration of ATP, counterclockwise rotation of the filament (viewed from the membrane) was observed (Fig. 1 *a* and *b*). Similar to the thermophilic enzyme (13), rotations often stopped for a variable time and then started again. The rotation required ATP and was inhibited by the addition of 1 mM azide, an inhibitor of F_1-ATPase (Fig. 1*c*).

The rotations became slower with an increase in the filament length. The degree of scatter of the experimental points was similar to that for the thermophilic enzyme (refs. 31 and 32; Fig. 2). The scatter may be partly due to the intrinsic property of the single-molecule catalysis.

From the scatter of experimental points, it was difficult to determine the torque generated by the enzyme precisely. Rotational rates were calculated assuming a constant torque of 30 and 80 pN·nm, corrected for ATPase turnover, and plotted as a function of filament length (Fig. 2, red and blue dotted lines, respectively). Most of the experimental points are between these two lines, indicating that F_1 produced apparent torque between 30 and 80 pN·nm to overcome the friction. Least square fitting of the experimental points gave an average frictional torque of ≈50 pN·nm. The free energy of ATP hydrolysis (Δ*G*ATP) is ≈80 pN·nm under physiological conditions and is comparable with the torque value $\times 2\pi/3$ (work done in one-third of a revolution), indicating that the thermodynamic efficiency is close to 100%, as shown for the thermophilic enzyme (31).

The rotational rate value of the γ-subunit without an actin filament may be consistent with the steady-state turnover rate of ATPase. As the rotational rate of the shortest filament observed (1 μm) is about ≈10 sec^{-1}, the rate without the filament may be ≈10–20 sec^{-1}, as estimated from Fig. 2. On the other hand, the rate of ATPase is ≈60 sec^{-1} (Table 1),

Table 1. ATPase activity of *E. coli* F_1 engineered for rotation

Enzyme	F_1-ATPase activity, s^{-1}
Nonengineered (wild-type)	55
αHis-tag/γS193C	64
αHis-tag/γS193C/γM23K	36

The ATPase activity (multisite rate, sec^{-1}) of the engineered (αHis-tag/γS193C) enzyme with or without the γM23K mutation, or the nonengineered (wild-type) enzyme was assayed at 25°C under the conditions (pH 7.2) used for rotation assays in the presence of 1 mM ATP/0.5 mM $MgCl_2$/0.2 mM NADH/20 μg/ml lactate dehydrogenase. Assays were started with the addition of 10 nM F_1.

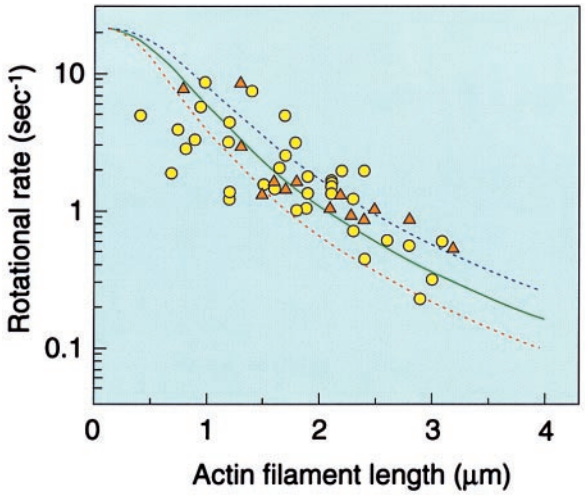

FIG. 2. Effect of the actin filament length on the rotational rate. Rates were estimated from the results giving more than five continuous rotations and are expressed as rotations per second. The reaction mixture was either 5 mM Mg-ATP (circles) or 0.5 mM Mg-ATP (triangles). Frictional torque was calculated with $(4\pi/3)\omega\eta L^3/[\ln(L/2r) - 0.447]$, where ω = angular velocity, $\eta(10^{-3}$ N·sec·$m^{-2})$ = the viscosity of the medium; L = length of the actin filament; and r (5 nm) = the radius of the actin filament (31, 36). Solid and dotted lines represent calculated rotational rates of the filaments with constant torque corrected for ATPase turnover: $\omega/2\pi = 1/3 \cdot 1/(\tau ATP + \tau step)$, where $1/\tau ATP$ is the turnover rate of ATPase and $\tau step$ is the time for 120° rotation with load. Rotational rates were calculated assuming three different torque values: red dotted line, 30 pN·nm; blue dotted line, 80 pN·nm; solid green line, least square fitting of the experimental points gave an average torque value of ≈50 pN·nm.

giving the approximate value of one rotation per three ATP hydrolysis.

Rotation and Torque Generation by the γM23K Mutant. F_0F_1 may be uncoupled if the γ-subunit can rotate but cannot

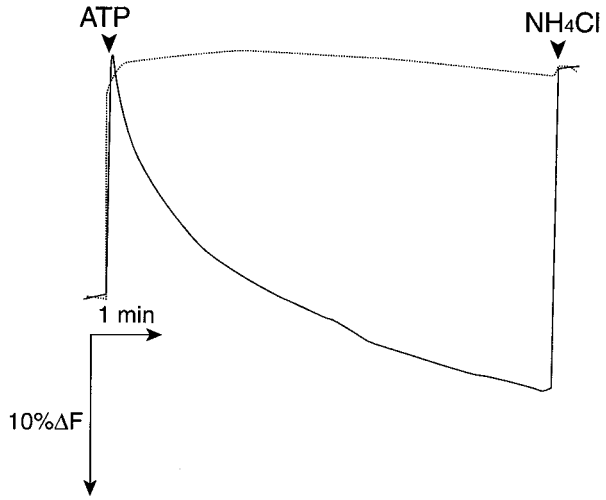

FIG. 3. ATP-dependent formation of an electrochemical proton gradient in membrane vesicles containing the engineered F_OF_1 with or without the γM23K mutation. ATP-dependent fluorescence quenching in membrane vesicles containing the engineered enzyme with (dotted line) or without (solid line) the γM23K mutation. Membrane vesicles (100 μg of protein) were suspended in the reaction mixture for the rotation assay containing 2 μM acridine orange. Fluorescence (F) at 530 nm was monitored at 25°C. At the time indicated (arrowhead), 10 μl of 100 mM ATP (1 mM final concentration) or 10 μl of 1 M NH_4Cl (10 mM) was added. Essentially the same results were obtained with 6 mM ATP and 2 μM quinacrine. Note that measurements were carried out under the conditions for the rotation assay.

generate enough torque to drive proton transport. Thus, it became of interest to study the rotation of an actin filament connected to the γ-subunit of an energy-coupling mutant. We selected the γM23K mutant for this study, because it is severely defective in energy coupling (22, 23). The mutation was introduced into the engineered enzyme, and ATPase activity and proton translocation were assayed under the conditions used for the rotation. The γM23K mutant enzyme showed essentially no proton translocation dependent on ATP hydrolysis (Fig. 3) but had about 60% of the wild-type ATPase activity (Table 1).

The actin filament connected to the mutant γ-subunit could rotate (Fig. 4*a*), and plots of rotational rates versus filament length were essentially the same as those of actin filaments connected to γ-subunits without the mutation (see Fig. 4*b*, for comparison). As most experimental points are above the curve calculated assuming a constant torque of 30 pN·nm (Fig. 4*a*, red dotted line), $2\pi/3 \times 30$ pN·nm (≈60 pN·nm) is the minimal estimate of the work done in one-third of a revolution. Dividing the estimate by ΔGATP (≈80 pN·nm) gives a minimal efficiency of ≈80%. The rotational rate without the filament was estimated to be ≈10–20 sec^{-1}, similar to the value for the wild type. These results suggest that the mutant enzyme can transform the chemical energy into mechanical work essentially just as the wild type does.

DISCUSSION

In the present study, ATP-dependent rotation of an actin filament connected to the *E. coli* γ-subunit was observed directly, with a scatter of experimental points similar to that of thermophilic *Bacillus* PS3 (3, 13, 31). The estimated rotational rate of the γ-subunit without a filament and ATPase turnover were consistent with one rotation per three ATP hydrolyzed, as predicted by the binding-change mechanism (5). The estimated frictional torque confirms the thermodynamic calculation, indicating that the efficiency of energy transduction (mechanical work per free energy of ATP hydrolyzed) is nearly 100% (31).

In the binding-change mechanism (5), catalysis is coupled to proton transport by a subunit complex extending through F_0F_1. During ATP synthesis, proton movement rotates the assembly of *c*, γ, and ε and changes the conformations of the catalytic sites successively to release product ATP. In the reverse reaction, ATP hydrolysis rotates the γ-subunit and possibly the *c* subunit oligomer to complete ATP-dependent proton trans-

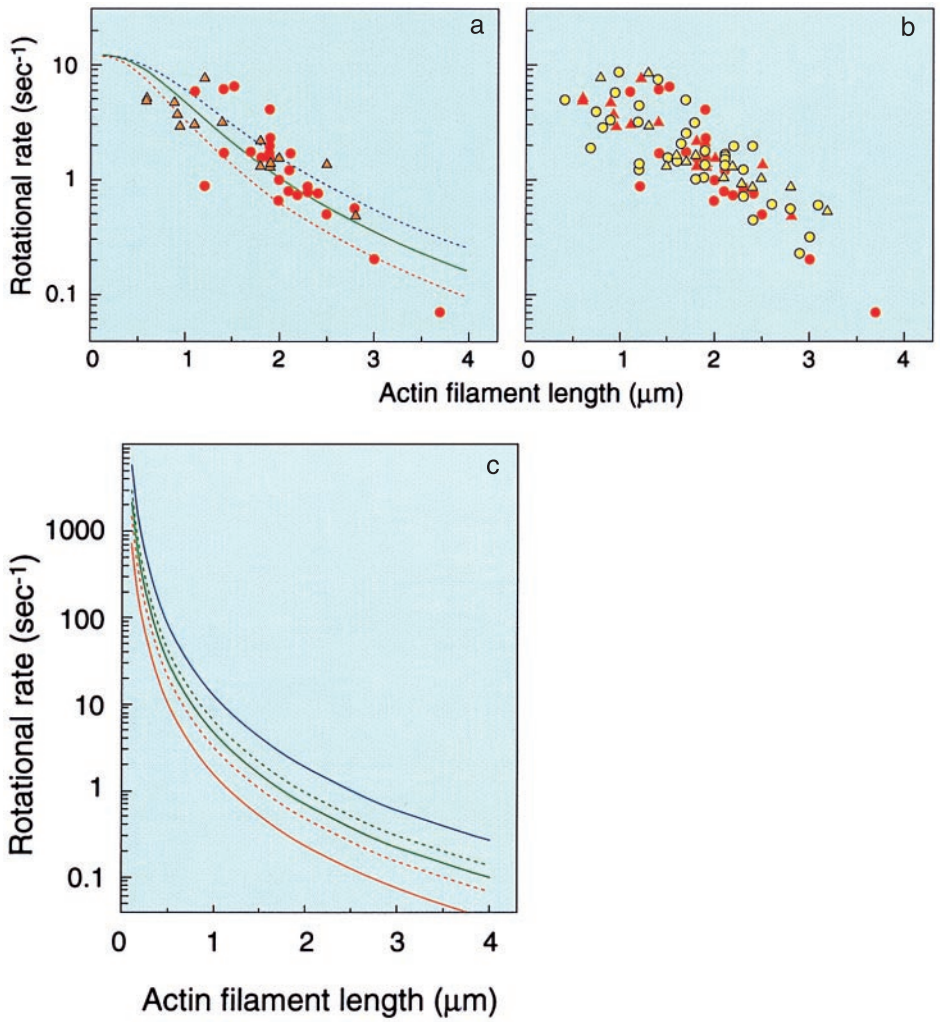

FIG. 4. Rotation of an actin filament attached to the engineered F_1-ATPase with the γM23K mutation. (*a*) Rotation of the γM23K γ-subunit was recorded in the presence of 5 mM Mg-ATP (circles) or 0.5 mM Mg-ATP (triangles). Lines represent calculated rotational rates of the filaments with constant torque corrected for ATPase turnover: red dotted line, 30 pN·nm; blue dotted line, 80 pN·nm; solid green line, least square fitting of the experimental points gave an average torque of ≈50 pN·nm. Rotational rates were estimated as described in the legend to Fig. 2. (*b*) Rotational rates of γM23K subunit (red) are plotted together with those of the wild-type subunit (yellow) for direct comparison. (*c*) Calculated rotational rates of the filaments with constant torque not corrected for ATPase turnover are shown: red solid line, 10 pN·nm; red dotted line, 20 pN·nm; green solid line, 30 pN·nm; green dotted line, 40 pN·nm; blue solid line, 80 pN·nm. See legend to Fig. 2 for calculation.

port. Rotation of the *c* subunit oligomer has been proposed (5, 12, 14), and that of $\gamma\varepsilon$ relative to the $\alpha 3\beta 3$ assembly in F_OF_1 has been suggested by cross-linking experiments (33, 34). Therefore, the ATP-dependent rotation observed in the $\alpha 3\beta 3\gamma 1$ complex or F_1 may be a part of the movement of the $c\gamma\varepsilon$-assembly. However, it is not known whether the $c\gamma\varepsilon$-assembly rotates simultaneously or whether rotation of $\gamma\varepsilon$ is transmitted to the *c* subunit oligomer. Such questions regarding the coupling mechanism between catalysis, mechanical work, and proton transport could be answered by studying *E. coli* ATP synthase, taking advantage of the accumulated genetic and biochemical information.

As described above, the rotational rate of the γ-subunit in F_1 is consistent with a constant frictional torque, when long actin filaments (>1 μm) are attached. For example, the rate with a 2-μm filament, calculated assuming constant torque of 40 pN·nm, gives a rotational rate of 0.92 sec^{-1}, almost similar to experimental values ($\approx$0.97–1.7 sec^{-1}). When the filament length becomes shorter than 1 μm, the same calculation gives much faster rotational rates. For example, the rates of a 0.1-μm filament, calculated with constant torque of 10 and 40 pN·nm are 1,400 and 2,800 sec^{-1}, respectively (Fig. 4*c*). However, these values could not be obtained experimentally for F_1, because the rates should be restricted by ATPase turnover at a catalytic site ($\approx$20 sec^{-1}). The rotations of the γ-subunit in F_1 become almost independent of torque, when the load becomes lighter (see Fig. 2 or 4, for calculated curves). Thus, it is possible that an uncoupled mutant F_1 has wild-type activity and rotation but generates lower torque, which is not sufficient to drive proton transport in F_OF_1. The γ-subunit rotation of such a mutant may not be strictly obligatory for ATPase activity, as evidenced by the thermophilic $\alpha 3\beta 3$ complex having significant ATPase activity (25% of $\alpha 3\beta 3\gamma$; ref. 35). Based on these considerations, we were interested in the γM23K mutant showing drastically inefficient energy coupling between ATPase catalysis and proton translocation (23). This study clearly showed that regardless of the mutation, the γ-subunit produced the same frictional torque, indicating that the energy generated by ATP hydrolysis in the wild type and mutant was converted to the mechanical work with similar efficiency.

These results suggest that the torque generated in F_OF_1 by the γ-subunit rotation should be transmitted to the *c* subunit oligomer to complete ATP-dependent proton translocation and that the γM23K enzyme is defective in such a transmission step. Conversely, ATP synthesis by the γM23K is defective possibly because proton transport through F_O is not coupled to the γ-subunit rotation. From the thermodynamic analysis, Al-Shawi *et al*. (25) showed that the γM23K mutant is defective in communication between F_1 and F_O via ε-subunit. Consistent with their results, our observation suggests that mutant enzyme is defective in the coupling process at the interface between F_1 and F_O.

The *E. coli* experimental system established in this study will contribute to a further understanding of the catalysis and energy coupling of ATP synthase. A future study should investigate whether the *c* subunit oligomer in F_OF_1 can rotate.

We thank Dr. Robert K. Nakamoto and Dr. Ashley Spies for critical reading of the manuscript. This work was supported in part by the Japanese Ministry of Education, Science, and Culture.

1. Futai, M., Noumi, T. & Maeda, M. (1989) *Annu. Rev. Biochem.* **8,** 111–136.
2. Futai, M. & Omote, H. (1996) in *Handbook of Biological Physics*, eds. Konings, W. N., Kaback, H. R. & Lolkema, J. S. (Elsevier, Amsterdam), Vol. 2, pp. 47–74.
3. Weber, J. & Senior, A. E. (1997) *Biochim. Biophys. Acta* **1319,** 19–58.
4. Fillingame, R. H. (1996) *Curr. Opin. Struct. Biol.* **6,** 491–498.
5. Boyer, P. D. (1997) *Annu. Rev. Biochem.* **66,** 717–749.
6. Penefsky, H. S. & Cross, R. L. (1991) *Adv. Enzymol. Relat. Areas Mol. Biol.* **64,** 173–214.
7. Abrahams, J. P., Leslie, A. G. W., Lutter, R. & Walker, J. E. (1994) *Nature (London)* **370,** 621–628.
8. Gogol, E. P., Johnston, E., Aggeler, R. & Capaldi, R. A. (1990) *Proc. Natl. Acad. Sci. USA* **87,** 9585–9589.
9. Aggler, R., Haughton, N. A. & Capaldi, R. A. (1995) *J. Biol. Chem.* **270,** 9185–9191.
10. Duncan, T. M., Bulygin, V. V., Zhou, Y., Hutcheon, M. L. & Cross, R. L. (1995) *Proc. Natl. Acad. Sci. USA* **92,** 10964–10968.
11. Sabbert, D., Engelbracht, S. & Junge, W. (1996) *Nature (London)* **381,** 623–625.
12. Junge, W., Lill, H. & Engelbrecht, S. (1997) *Trends Biochem. Sci.* **22,** 420–423.
13. Noji, H., Yasuda, R., Yoshida, M. & Kinoshita, K., Jr. (1997) *Nature (London)* **386,** 299–302.
14. Vik, S. B. & Antonio, B. J. (1994) *J. Biol. Chem.* **269,** 30364–30369.
15. Omote, H., Maeda, M. & Futai, M. (1992) *J. Biol. Chem.* **267,** 20571–20576.
16. Park, M.-Y., Omote, H., Maeda, M. & Futai, M. (1994) *J. Biochem.* **116,** 1139–1145.
17. Senior, A. E. & Al-Shawi, M. K. (1992) *J. Biol. Chem.* **267,** 21471–21478.
18. Senior, A. E., Wilke-Mounts, S. & Al-Shawi, M. K. (1993) *J. Biol. Chem.* **268,** 6989–6994.
19. Amano, T., Hisabori, T., Muneyuki, E. & Yoshida, M. (1996) *J. Biol. Chem.* **271,** 18128–18133.
20. Löbau, S., Weber, J., Wilke-Mounts, S. & Senior, A. E. (1997) *J. Biol. Chem.* **272**, 3648–3656.
21. Iwamoto, A., Miki, J., Maeda, M. & Futai, M. (1990) *J. Biol. Chem.* **265,** 5043–5048.
22. Shin, K., Nakamoto, R. K., Maeda, M. & Futai, M. (1992) *J. Biol. Chem.* **267,** 20835–20839.
23. Nakamoto, R. K., Maeda, M. & Futai, M. (1993) *J. Biol. Chem.* **268,** 867–872.
24. Nakamoto, R. K., Al-Shawi, M. & Futai, M. (1995) *J. Biol. Chem.* **270,** 14042–14046.
25. Al-Shawi, M. K., Ketchum, C. J. & Nakamoto, R. K. (1997) *J. Biol. Chem.* **272,** 2300–2306.
26. Jeanteur-de Beukelar, C., Omote, H., Iwamoto-Kihara, A., Maeda, M. & Futai, M. (1995) *J. Biol. Chem.* **270,** 22850–22854.
27. Klionsky, D. J., Brusilow, W. S. A. & Simoni, R. D. (1984) *J. Bacteriol.* **160,** 1055–1060.
28. Omote, H., Tainaka, K., Fujie, K., Iwamoto-Kihara, A., Wada, Y. & Futai, M. (1998) *Arch. Biochem. Biophys.* **358,** 277–282.
29. Harada, Y., Sakura, K., Aoki, T., Thomas, D. D. & Yanagida, T. (1990) *J. Mol. Biol.* **216,** 49–68.
30. Hartman, H., Syvanen, M. & Buchanan, B. B. (1990) *Mol. Biol. Evol.* **7,** 247–254.
31. Yasuda, R., Noji, H., Kinoshita, K., Jr., & Yoshida, M. (1998) *Cell* **93,** 1117–1124.
32. Kato-Yamada, Y., Noji, H., Yasuda, R., Kinoshita, K., Jr., & Yoshida, M. (1998) *J. Biol. Chem.* **273,** 19375–19377.
33. Aggeler, R., Ogilvie, I. & Capaldi, R. A. (1997) *J. Biol. Chem.* **272,** 19621–19624.
34. Zhou, Y., Duncan, T. M. & Cross, R. (1997) *Proc. Natl. Acad. Sci. USA* **94,** 10583–10587.
35. Kagawa, Y., Ohta, S. & Otawara-Hamamoto, Y. (1989) *FEBS Lett.* **249,** 67–69.
36. Hunt, A. J., Gittes, F. & Howard, J. (1994) *Biophys. J.* **67,** 766–781.